Original Article

Effect of Mercuric Chloride Exposure during Pregnancy and Lactation on the Postnatal Development of the Liver in the Albino Rat

Mohamed El-Badry Mohamed, Manal M.S. El-Meligy, Reneah R. Bushra and Esraa K. Mohamed

Department of Human Anatomy and Embryology, Faculty of Medicine, Assiut University, Assiut, Egypt

ABSTRACT

Background: Mercury (Hg) is a prominent environmental contaminant that causes detrimental effects to the human health. It is used in some thermometers, electrical switches, batteries, fluorescent lamps, paints, fungicides, insecticides and in mercuric vapours lamps. Mercury and its compounds have been also used in medicine as in topical antiseptics, stimulant laxatives, skin lightening products, diaper rash ointment, eye and nasal sprays. Elemental mercury is an ingredient in dental amalgams. Thiomersal (mercury-based preservative) is an organic compound that is used as a preservative in vaccines and in the manufacture of mascara.

Aim of the Work: To detect the effects of mercuric chloride ($HgCl_2$) exposure during pregnancy and lactation on the postnatal development of the liver in albino rat.

Materials and Methods: A total number of sixteen pregnant albino rats were used in the study. They were equally divided into control and experimental groups. During the whole periods of gestation and lactation, the control females received an oral daily saline of 2 mg /kg body weight. The experimental females received an oral daily dose of 2 mg $HgCl_2$ /kg body weight. After weaning, the offspring of the treated group was given $HgCl_2$ of the same oral daily dose. The control and treated mothers' offspring was sacrificed at the following ages: 1 day (group I), 21 days (group II) and 2 months (group III). Each group consisted of 6 rats. At the time of scarification, the rats were weighed, anaesthetized and the livers were extracted and weighed. The specimens from the fixed livers were dissected and processed for the light and the electron microscopic examination. Morphometric studies were also done.

Results: Light microscopic study of the treated groups revealed vacuolization, degeneration of the hepatocytes, inflammatory cell infiltration, dilated and congested hepatic sinusoids as well as portal venules. Weak PAS reaction was observed in the treated liver specimens of groups I and II and a strong PAS reaction in the treated group III when compared with the corresponding controls. The electron microscopic study showed degeneration of the mitochondria, vacuolization of the cytoplasm, congested sinusoids with perisinusoidal fibrosis. Morphometric studies revealed a significant increase in the liver weight inspit of the decrease in the body weight.

Conclusion: Ingestion of $HgCl_2$ during pregnancy and lactation produces hepatic affections of the offspring.

Received: 01 July 2017, **Accepted:** 03 August 2017

Key Words: Albino rat, liver, mercuric chloride.

Corresponding Author: Mohamed El-Badry Mohamed, Department of Human Anatomy and Embryology, Faculty of Medicine, Assiut University, Assiut, Egypt, **Tel.:** +20 1283553122, **E-mail:** melbadry_55@hotmail.com

The Egyptian Journal of Anatomy, ISSN: 0013-2446, Vol. 42 No. 1

 DOI:10.21608/EJANA.2022.249442

INTRODUCTION

The liver is the largest internal organ in the body and it functions as both an exocrine and endocrine gland ***(Tayeb et al., 2010)***. The functions of the liver include destruction of the aged red blood cells, synthesis and secretion of the bile as well as plasma lipoproteins and storage of glycogen and lipids ***(Rui, 2014)***. The structural unit of the liver has been considered to be the hepatic lobule ***(Krishna, 2013)***.

Mercury is the only metallic element that is liquid at the standard conditions for temperature and pressure. The natural events like volcanic activity and human activities like mining, fuel use, coal burning for heating and cooking, industrial processes and waste incinerators can cause mercury releases into the environment. The natural processes can also change mercury from one form to another ***(Rustagi and Singh, 2010; Liu et al., 2012)***.

Mercury exists in nature in elemental, inorganic and organic forms ***(Robin, 2012; Blum, 2013)***. It has been used primarily for the manufacture of industrial chemicals, thermometers, electrical switches, batteries, fluorescent lamps and in mercuric vapours lamps. Mercury and its compounds have been also used in medicine as in topical antiseptics, laxatives, skin lightening products, diaper rash ointment, ingredient in dental amalgams and nasal sprays. Thiomersal-mercuric based compound- is used as a preservative in vaccines ***(Guzzi and La Porta, 2008)***.

Generally, two groups are more sensitive to the effects of mercury. The first group is thee fetuses who are the most susceptible to developmental effects due to mercury. The second group is the people who are regularly exposed to high levels of mercury such as the populations that rely on subsistence fishing or people who are occupationally exposed ***(O`Reilly et al., 2010)***.

MATERIALS AND METHODS

Chemicals

$HgCl_2$ was purchased in a powder form from El-Gomhouria Company for Trading Chemicals and Medical Appliances, Assuit.

Animals

A total number of 16 (180-200g) adult female rats were used in this study. They were being pregnant after overnight mating with 4 (200-250g) adult male albino rats (one male for four female rats). The presence of sperms in the vaginal plug on light microscopic examination was recorded as 0 day pregnancy ***(Mahmoud and El-Badry, 2001)***. The animals were obtained from the Animal House, Assiut University. The experiment was approved by the Institutional Ethics Committee of Assiut University.

Experimental design

The pregnant rats were singly housed and divided randomly into control and experimental groups (each consisted of 8 rats).

The pregnant rats of the experimental compartment received $HgCl_2$ in an oral daily dose of 2 mg/kg body weight through a gastric tube during the periods of gestation and lactation ***(Mohamed et al., 2010)***. After weaning, the offspring of the treated group was given $HgCl_2$ in an oral daily dose of 2 mg/kg body weight. The control compartment was given normal saline via the same route, dose and for the same periods. A number of 6 offspring of the control rats and the same number of their experimental control were selected at the following ages:

- 1 day (group I)
- 21 days (group II)
- 2 months (group III)

At the time of scarification, all groups were weighed, anaesthetized by ether inhalation, subjected to an intracardiac perfusion by normal saline 0.9% NaCl then sacrificed. Liver specimens were extracted from the different groups and weighed. The specimens were put in a suitable fixative solution for further processing.

Light microscopic study

The liver specimens were fixed in 10% formalin then processed for paraffin blocks. The liver specimens were subjected for Haematoxyline and eosin (Hx&E) stain ***(Kyriacos et al., 2013)*** and Periodic Acid Schiff (PAS) stain ***(Rastogi, 2009)***.

Electron Microscopic study

Liver tissue was dissected in about 3mm3 to allow electrons to pass right through the sample. Primary fixation was done in 2.5% glutaraldhyde+4% formaldehyde for 2 hours at room temperature. Fixative was washed in distilled water (DH_2O) 3 times in 10 minutes changes. Post Fixative was added in 1% Osmium Tetroxide for

1 hour. Fixative was washed out in DH_2O 3 times in 10 minutes changes. Dehydration Series were done as follows: 30% ethanol for 10 minutes, 50% ethanol for 10 minutes, 70% ethanol for 10 minutes, 90% ethanol for 10 minutes and 100% ethanol for 10 minutes, respectively ***(Kue, 2007)***.

Samples were embedded in fresh resin and cured overnight at 60°C. Sectioning process was done to produce thin slices of specimen which were cut on an ultramicrotome with a diamond knife to produce ultra-thin sections of 60-90 nm thick. The sections were stained for several minutes by double staining technique, with an aqueous or alcoholic solution of uranyl acetate followed by aqueous lead citrate ***(Kue, 2007)***. The sections were observed with the transmission electron microscope (TEM) ("Jeol" E.M.-100 CX11; Japan) at the Electron Microscopic Unit of Assiut University.

Morphometric study

Using computerized assisted image analysis, the hepatocytes nuclei diameters were measured. The data were collected and analyzed using SPSS program (version 16.0). A statistical analysis to compare control and treated measurements was performed using the Mann-Whitney Test ***(Levesque, 2007)***.

RESULTS

Light microscopic study

Group I

Hx&E specimens of the control rats showed polygonal hepatocytes arranged in radiating cords of two cells thickness from the central veins towards the periphery of the hepatic lobules. The nuclei were large dense centrally placed (Figures 1,2). Hepatic sinusoids showed few blood cells (Figure 2).

Specimens of the treated rats showed the same arrangement of the hepatocytes but the cords were separated from each other by wider hepatic sinusoids with intact endothelial lining (Figure 4). The hepatic nuclei were large dense centrally placed (Figures 4,5). The cytoplasm of the hepatocytes showed multiple vacuolated areas (Figures 4,5). Large number of fat cells appeared between the hepatocytes (Figure 5). Large number of inflammatory cells infiltrated between the hepatocytes. The portal vein was dilated but of intact outline. Both portal vein and bile ducts were surrounded by inflammatory cells. Ito cells appeared adjacent to the sinusoids (Figure 4).

Using PAS stain, the cytoplasm of the hepatocytes showed dark red granules indicating PAS positive reaction which was weaker in the treated rats (Figure 6) in comparison to the control ones (Figure 3).

Group II

Hx&E specimens of the control rats showed cords of less polygonal hepatocytes. The cords were separated from each other by the radically arranged sinusoids. The hepatocytes were of rounded well-defined nuclei. The hepatic nuclei were centrally placed. The portal venules were of intact regular outline (Figure 7).

On the other hand, specimens of the treated rats showed variable degrees of architecture disorganization. Some hepatocytes were swollen and their cytoplasm was apparently vacuolated. Others were degenerated cells leaving patchy necrotic areas within the hepatic lobules. The cords of hepatocytes were separated from each other by wide hepatic sinusoids. The central veins had damaged endothelial lining and were irregular, dilated and of blood cell content. Prominent nuclei of Kupffer cells were detected (Figure 9).

Using PAS stain, the cytoplasm of the hepatocytes showed dark red granules indicating PAS positive reaction which was weaker in the treated rats (Figure 10) in comparison to the control ones (Figure 8).

Group III

Hx&E specimens of the control rats showed cords of polygonal hepatocytes of one cell thickness separated from each other by hepatic sinusoids. The hepatic sinusoids were of intact endothelial lining. Hepatic nuclei were large, rounded and centrally placed (Figures 11,12). Their nucleoli were prominent (Figure 12). Some hepatocytes were binucleated. Scattered few lymphocytes appeared surrounding the central veins (Figure 11). The portal tract field showed portal venule and bile ductules. The portal venule was regular and of intact lining (Figure 12).

On the other hand, specimens of the treated rats showed cords of less polygonal hepatocytes separated from each other by relatively wide sinusoids (Figure 14). Hepatocytes were swollen (Figures 14,15). Some hepatic nuclei were less rounded but others were polymorphic (Figures 14,15). The cytoplasm was vacuolated especially at the periphery of the cell

(Figures 14,15). The central veins were irregular, dilated and congested with blood and inflammatory cells infiltrate nearby. Their endothelial lining was destructed (Figure 14). The portal tract field showed distorted and congested portal venules and dilated irregular bile ductules. The portal tract region was surrounded by inflammatory cells (Figure 15). Prominent nuclei of von Kupffer cells were observed (Figures 14,15).

Using PAS stain, the cytoplasm of the hepatocytes showed dark red granules indicating PAS positive reaction which was stronger in the treated rats (Figure 16) in comparison to the control ones (Figure 13).

Electron microscopic study

Group I

Ultrastructural cross section of the controls showed hepatocytes of ill defined borders with centrally placed rounded nuclei and prominent nucleoli. The cytoplasm was filled with cell organelles (Figure 17).

On the other hand, specimens of the treated rats showed polygonal hepatocytes with apparent outline. The nucleus was large rounded with ill defined nucleolus. Marked loss of the cell organelles was noticed. The cytoplasm was highly vacuolated and the vacuolization process started at periphery of the cytoplasm. Variable sized scattered mitochondria appeared within the hepatocytes and some were degenerating. Large amount of lysosomes were noticed. Mitotic divisions of the hepatocyte were present but the newely formed cells were compressed by mild perisinusoidal fibrosis. Mercury deposits were scattered among the remaining cytoplasm (Figure 18).

Group II

Cross section of control liver showed polygonal hepatocytes of well-defined cell membranes with centrally placed rounded nuclei. Mitochondria were rounded, scattered and of relatively small size. Hepatic sinusoids were of intact lining and von Kupffer cells appeared lining the walls of the sinusoids (Figure 19).

In contrast, specimens of the treated livers showed less polygonal hepatocytes. Their nuclei were large rounded with ill defined nucleoli. Marked loss of the cell organelles was observed and the cytoplasm was highly vacuolated. Large amount of lysosomes appeared within the field. Some mitochondria were degenerated. Von Kupffer cells were abnormally shaped. The rest of the cell organelles were masked by the rarefied cytoplasm. Mercuric deposits appeared within the field (Figure 20).

Group III

Cross section of control liver showed polygonal hepatocytes of clear-defined cell membranes (Figure 21). The nuclei were large and rounded (Figures 21,22) with prominent nucleoli (Figure 21). Large number of small-sized rounded mitochondria were scattered among cell organelles. Excess rough endoplasmic reticulum (RER) was noticed. Lysosomes of variable sizes appeared within the cytosol (Figures 21,22). Von Kupffer cells appeared within the sinusoidal wall (Figure 21). Glycogen granules are organized in the form of rosette clusters (Figure 22).

In contrast, specimens of the treated group showed less polygonal hepatocytes. The nuclei were less rounded. Some hepatocytes were binucleated (Figure 23). The hepatocytes showed thickened cell membranes (Figure 23) but some cells were of thinned ill-defined ones (Figure 24). The cytoplasm was vacuolated with apparent loss of the cell organelles (Figures 23,24). Mitochondria were few and swollen (Figure 24). Also the presence of RER (Figure 24) and excess lysosomes of variable sizes were detected (Figures 23,24). The rest of the cell organelles were masked by the rarefied cytoplasm (Figures 23,24). Hepatic sinusoids were congested with blood cells (Figures 23,24) with apparent perisinusoidal fibrosis (Figure 24). Mercury deposits appeared within the hepatocytes (Figures 23,24). Von Kupffer cells were large and abnormally shaped (Figure 23).

Morphometric study

Body weight

Regarding body weight, insignificant difference was observed between both treated and control rats of group I. On the other hand, groups II and III showed a statistically significant decrease in the body weight of the treated rats in comparison to the control ones (Table 1).

Liver weight

All the treated groups showed statistically significant increase in the liver weight in comparison to the corresponding control ones (Table 1).

Hepatocytes nuclear diameter

Regarding the hepatocytes nuclear diameter, group I showed insignificant difference between both treated and control rats. On the other hand, groups II and III showed a statistically significant decrease in the nuclear diameter of the treated rats in comparison to the control (Table 2).

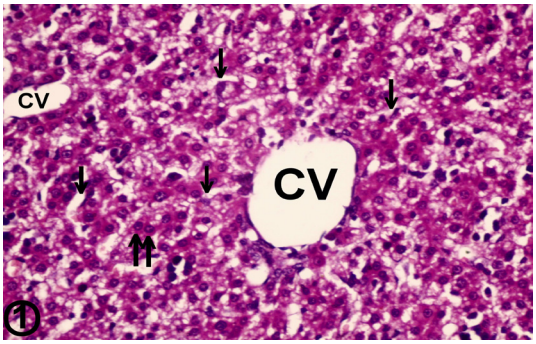

Fig. 1: A photomicrograph of a cross section of the rat liver (control group I) showing a central vein (CV) with cords of two hepatocytes thickness (double up arrows) radiating from it towards the periphery of the hepatic lobule. The cords are separated from each other by hepatic sinusoids (down arrows). (Hx & E ×400)

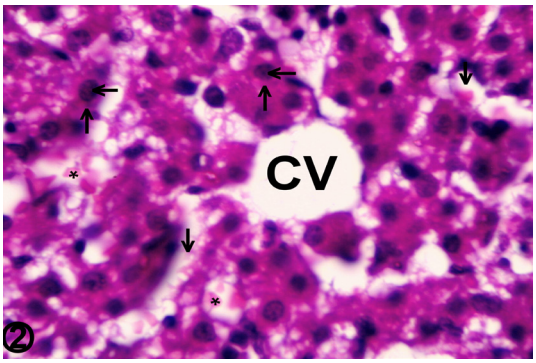

Fig. 2: A photomicrograph of cross section of rat liver (control group I) showing polygonal hepatocytes with eosinophilic cytoplasm (up arrows), large dense centrally placed rounded nuclei (left arrows) and hepatic sinusoids (down arrows) containing few blood cells (black stars). (Hx & E ×1000)

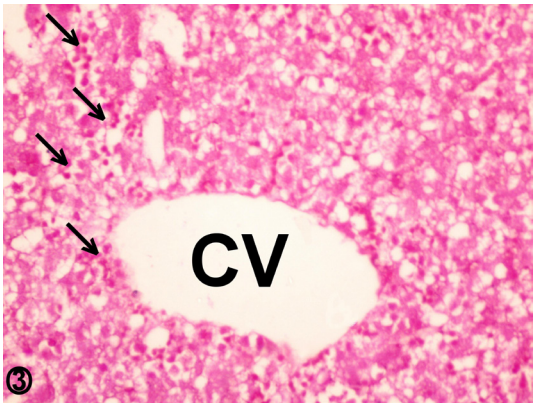

Fig. 3: A photomicrograph of cross section of rat liver (control group I) showing dark red granules (arrows) within the cytoplasm of the hepatocytes indicating PAS positive reaction. (PAS ×400)

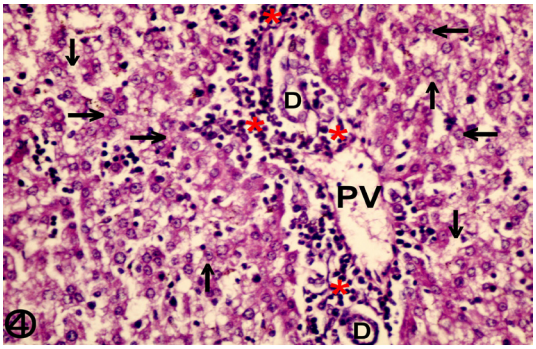

Fig. 4: A photomicrograph of a cross section of the rat liver (treated group I) showing a portal tract area. The portal venule (PV) is dilated but of intact outline. Both portal venule (PV) and bile ductules (D) are surrounded by massive inflammatory cells (red stars).The hepatocytes (up arrows) are arranged in cords which are separated from each other by wide hepatic sinusoids (down arrows). The hepatic nuclei are rounded and centrally placed (left arrows). The cytoplasm of the hepatocytes is vacuolated (right arrows). (Hx & E ×400)

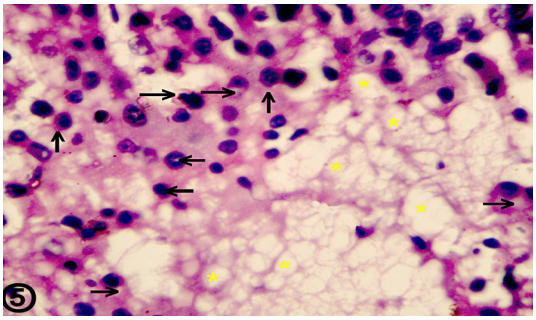

Fig. 5: A photomicrograph of a cross section of the rat liver (treated group I) showing cords of hepatocytes (up arrows) of normal architecture with large rounded nuclei (left arrows). The cytoplasm of the hepatocytes is vacuolated (right arrows). Large number of fat cells (yellow stars) appears between the cords. (Hx& E ×1000)

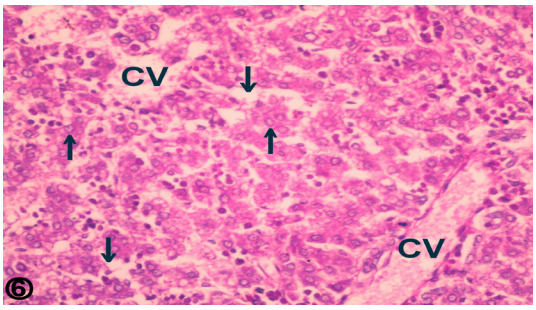

Fig. 6: A photomicrograph of a cross section of the rat liver (treated group I) showing cords of hepatocytes (up arrows) of normal architecture separated by hepatic sinusoids (down arrows). There is weaker PAS reaction of the hepatocytes in comparison to the control rats. (PAS ×400)

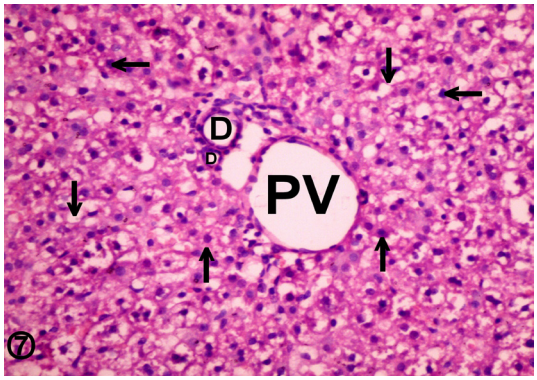

Fig. 7: A photomicrograph of a cross section of portal tract region of the rat liver (control group II) showing portal venule (PV) and bile ductules (D). Cords of hepatocytes (up arrows) radiating around and separated from each other by hepatic sinusoids (down arrows). The portal venule is of intact regular outline. The hepatocytes are less polygonal with rounded well-defined nuclei (left arrows). (Hx& E ×400)

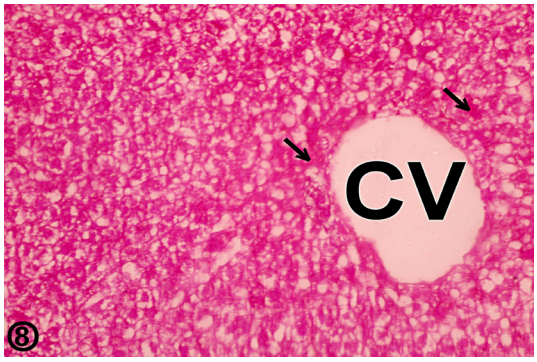

Fig. 8: A photomicrograph of a cross section of the rat liver (control group II) showing dark red material (arrows) within the cytoplasm of the hepatocytes indicating PAS positive granules. (PAS ×400)

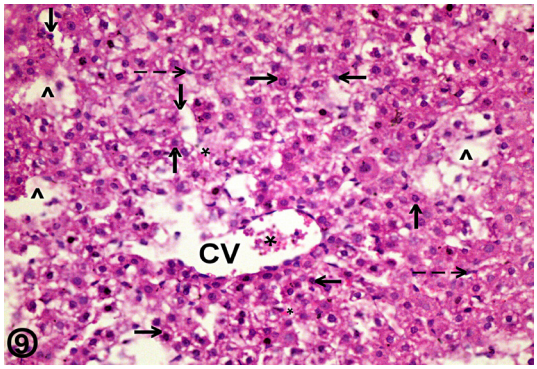

Fig. 9: A photomicrograph of a cross section of the rat liver (treated group II) showing obvious disorganization of hepatic architecture with patchy necrotic areas (arrow heads) within the hepatic lobules. The hepatocytes (up arrows) are swollen and the cytoplasm is apparently vacuolated (right arrows). Hepatic nuclei are polymorphic (left arrows). The central vein is damaged and contains blood cells (black stars). The hepatocytes are arranged in cords separated from each other by wide hepatic sinusoids (down arrows). Prominent nuclei of von Kupffer cells (interrupted right arrows) are observed. (Hx& E ×400)

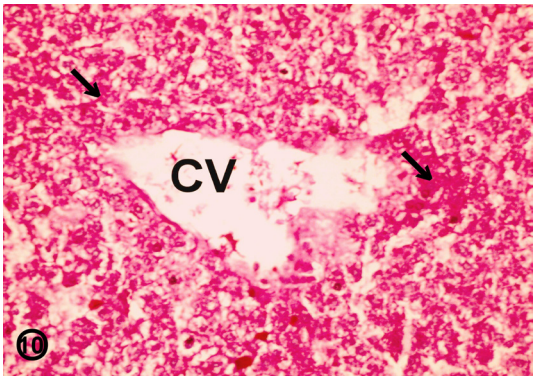

Fig. 10: A photomicrograph of a cross section of the rat liver (treated group II) showing destructed central vein (CV) with cords of irregularly shaped hepatocytes radiating from it. Rep purple material is observed within the cytoplasm (arrows). Weaker PAS reaction of the hepatocytes is noticed in comparison to the control rats. (PAS ×400)

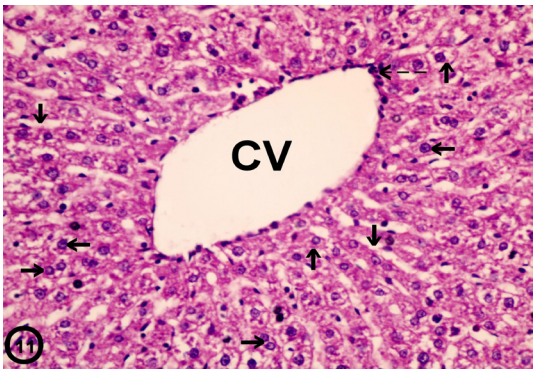

Fig. 11: A photomicrograph of a cross section of the rat liver (control group III) showing hepatocytes (up arrows) of the hepatic lobule radiating from the central vein (CV) in cords of one cell thickness separated from each other by sinusoids (down arrows). Hepatic nuclei are large, dense and centrally placed (left arrows). Some hepatocytes are binucleated (right arrows). Scattered few lymphocytes appear surrounding the central vein (interrupted left arrows). Both the central vein and the hepatic sinusoids are of intact endothelial lining. (Hx& E ×400)

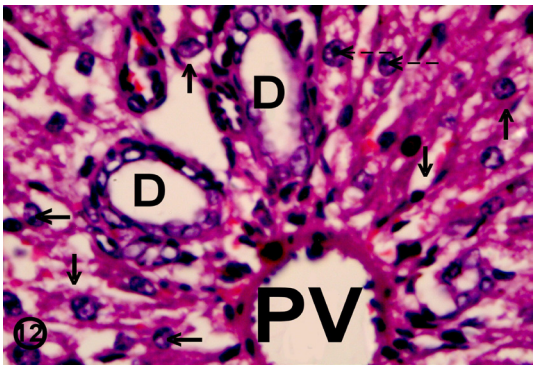

Fig. 12: A photomicrograph of a cross section of the portal tract of the rat liver (control group III) showing portal venule (PV) and bile ductules (D). Both are of intact lining as well as the hepatic sinusoids (down arrows). Hepatocytes (up arrows) are polygonal. Hepatic nuclei (left arrows) are large rounded with prominent dense nucleoli (interrupted left arrows). (Hx& E ×1000)

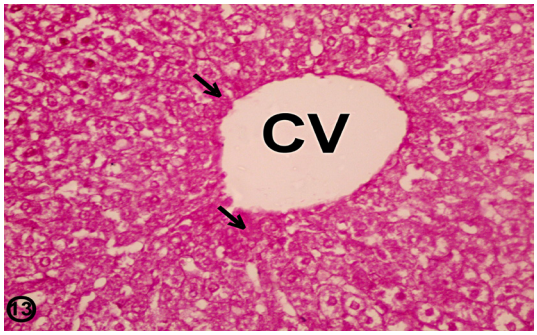

Fig. 13: A photomicrograph of a cross section of the rat liver (control group III) showing dark red material (arrows) within the cytoplasm of the hepatocytes indicating PAS positive granules. This red material appears more in the pericentral hepatocytes than the distal ones. (PAS ×400)

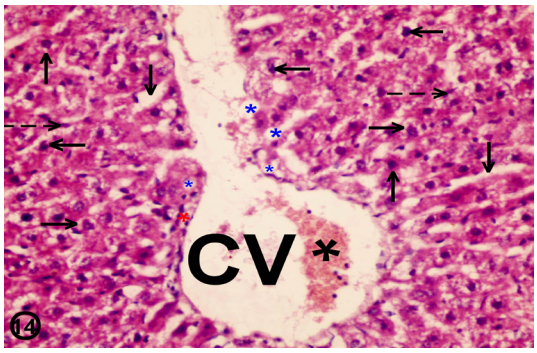

Fig. 14: A photomicrograph of a cross section of the rat liver (treated group III) showing cords of swollen hepatocytes (up arrows) arranged in cords from the central vein (CV) towards periphery of the hepatic lobule. They are separated from each other by relatively wide sinusoids (down arrows). Hepatic nuclei are polymorphic (left arrows) and the cytoplasm is apparently vacuolated (right arrows). The central vein is distorted and congested with blood cells (black stars). Large number of Ito cells (blue stars) appears within the persinusoidal space. Inflammatory cells (red stars) infiltrate near the central vein. Prominent nuclei of von Kupffer cells (interrupted right arrows) are observed. (Hx& E ×400)

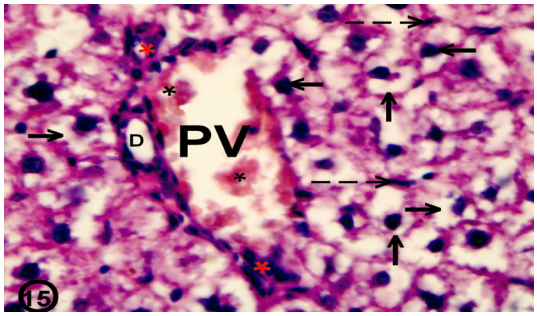

Fig. 15: A photomicrograph of a cross section of the rat liver (treated group III) showing swollen irregular hepatocytes (up arrows). Hepatic nuclei are polymorphic (left arrows) and the cytoplasm is markedly vacuolated (right arrows).The portal tract region is surrounded by inflammatory cells (red stars). The portal venule (PV) is destructed and congested with blood cells (black stars). The bile ductule (D) is relatively dilated. Prominent irregular nuclei of von Kupffer cells (interrupted right arrows) are observed. (Hx& E ×1000)

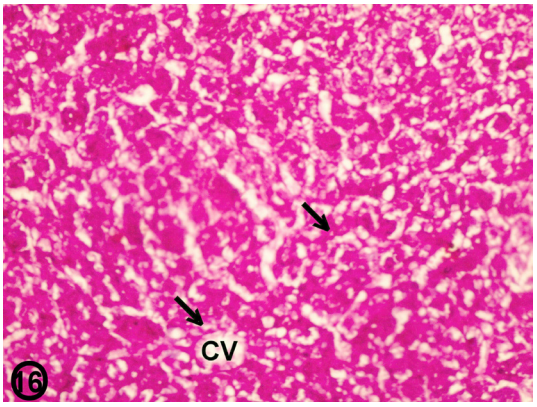

Fig. 16: A photomicrograph of a cross section of the rat liver (treated group III) showing stronger PAS reaction of the hepatocytes is noticed in comparison to the control rats. Cell borders of hepatocytes are indistinct. The red purple granules are equally distributed in both the pericentral and distal hepatocytes (arrows). (PAS ×400)

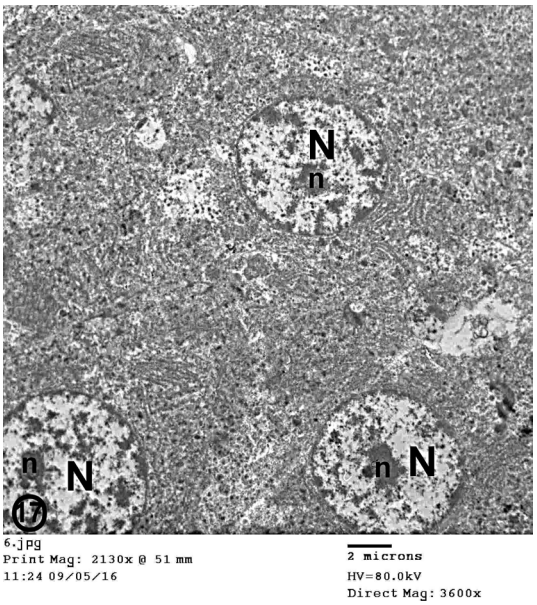

Fig. 17: A photomicrograph of cross section of rat liver (control group I) showing hepatocytes of ill defined borders with centrally placed rounded nuclei (N) and prominent nucleoli (n). The cytoplasm is filled with cell organelles. (TEM ×3600)

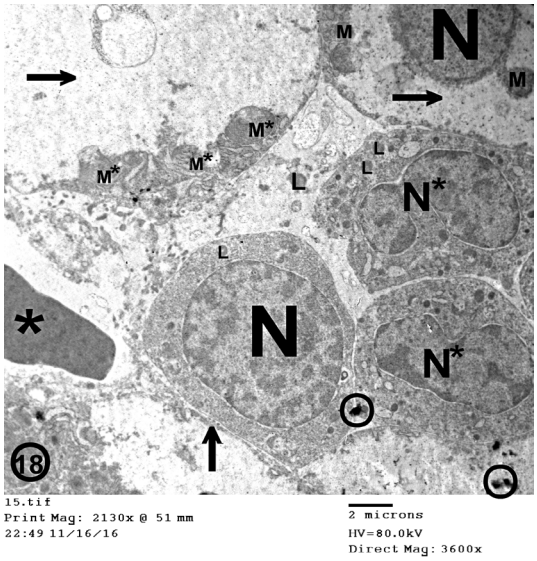

Fig. 18: A photomicrograph of a cross section of the rat liver (treated group I) showing adjacent hepatocytes of normal architecture. The nucleus (N) is large rounded with ill-defined nucleolus. Marked loss of the cell organelles was noticed. The cytoplasm is highly vacuolated (right arrows) and the vacuolization process started at periphery of the cytoplasm. Variable-sized scattered mitochondria (M) are present with large amount of lysosomes (L). Some mitochondria are degenerating (M*). Mitotic divisions of the hepatocytes are present (N*). The newly formed cells are compressed by mild perisinusoidal fibrosis (up arrows). Hepatic sinusoids are filled with blood cells (black stars). Mercuric deposits appear within the cytoplasm (circles). (TEM ×3600)

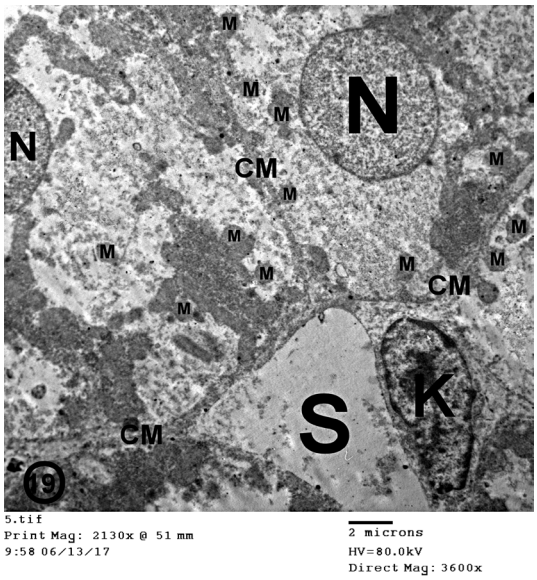

Fig. 19: A photomicrograph of a cross section of the rat liver (control group II) showing polygonal hepatocytes of well defined cell membranes (CM) with centrally placed rounded nuclei (N). Large number of mitochondria (M) appears rounded, scattered and of relatively small size. The hepatic sinusoid (S) is of intact lining and von Kupffer cell (K) lines its wall. (TEM ×3600)

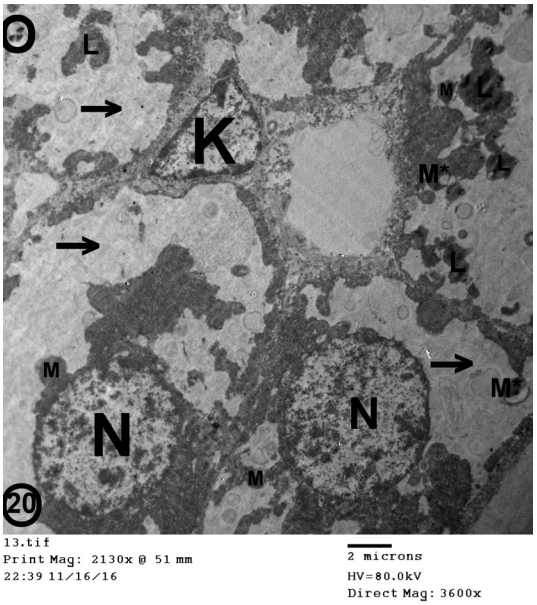

Fig. 20: A photomicrograph of a cross section of the rat liver (treated group II) showing adjacent hepatocytes with less polygonal outlines. The nuclei (N) are large rounded with ill-defined nucleoli. Marked loss of the cell organelles is observed. The cytoplasm is highly vacuolated (right arrows). Polymorphic mitochondria (M) appear within the cytoplasm with large amount of lysosomes (L). Some mitochondria are degenerated (M*). Von Kupffer cell (K) is abnormally shaped. Mercuric deposits appear within the field (circles). (TEM ×3600)

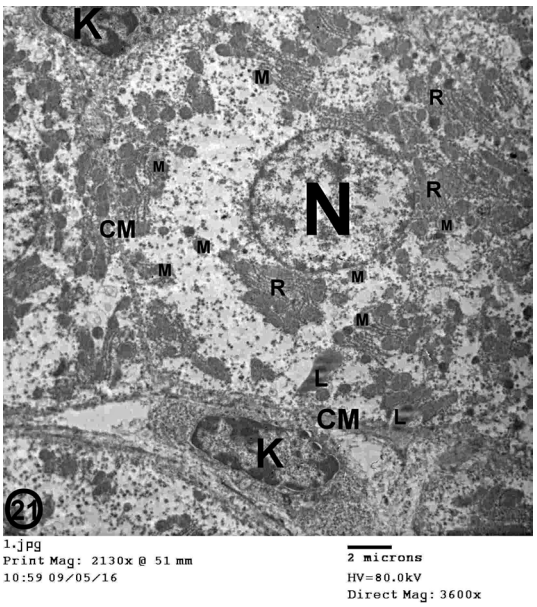

Fig. 21: A photomicrograph of a cross section of the rat liver (control group III) showing polygonal hepatocyte of clear defined cell membrane (CM). The nucleus (N) is large and rounded with prominent nucleolus (n). Well developed RER (R) is located. Large number of small sized mitochondria (M) is scattered among cell organelles. Few lysosomes are seen within the field (L).Von Kupffer cell (K) appears within the sinusoidal wall. (TEM ×3600)

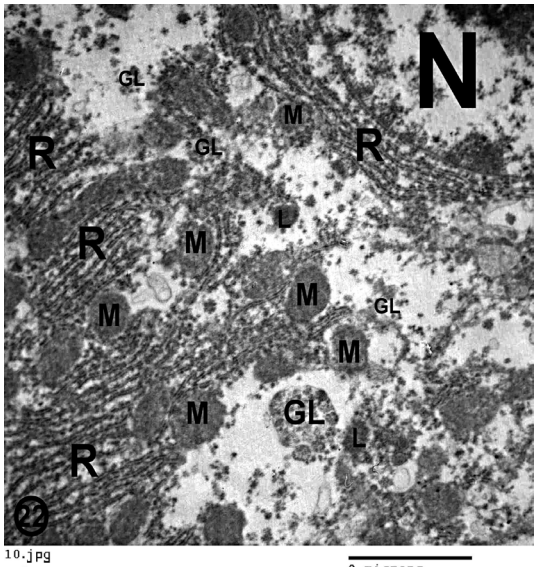

Fig. 22: A photomicrograph of a cross section of the rat liver (control group III) showing cell organelles of the hepatocyte located near the nucleus (N). Mitochondria (M) are rounded and scattered. Excess RER (R) is noticed. Glycogen granules (GL) are mainly organized in the form of rosette clusters. Lysosomes (L) appear within the cytosol. (TEM ×10000)

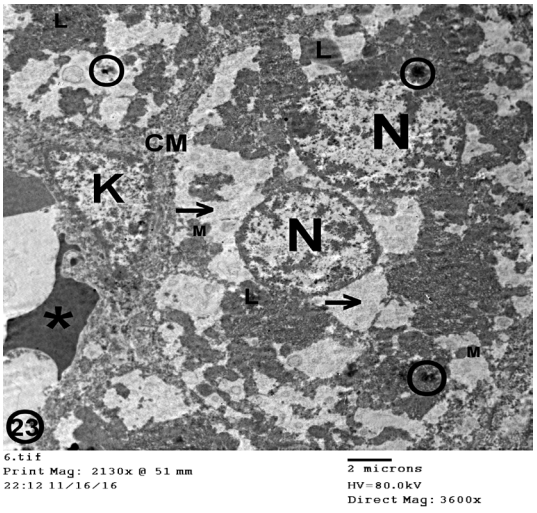

Fig. 23: A photomicrograph of a cross section of the rat liver (treated group III) showing less polygonal binucleated hepatocytes with thickened cell membrane (CM). The nuclei (N) are rounded with ill defined nucleoli and the cytoplasm is vacuolated (right arrows) with apparent loss of the cell organelles. Mitochondria (M) are few and small-sized. Some lysosomes are detected (L). Hepatic sinusoids are congested with blood (black stars).Von Kupffer cell (K) is large and abnormally shaped. Mercuric deposits appear within the field (circles). (TEM ×3600)

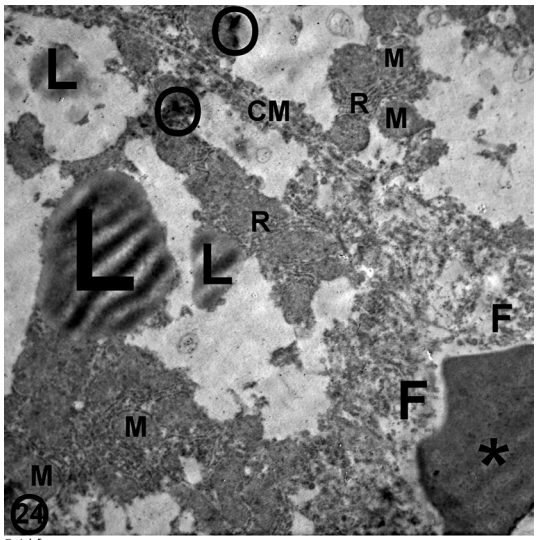

Fig. 24: A photomicrograph of a cross section of the rat liver (treated group III) showing the adjacent hepatocytes. The cell membrane (CM) is thinned. Mitochondria (M) are swollen with indistinct cristae. It also shows the presence of some RER (R) and large-sized irregularly-shaped lysosomes (L). Hepatic sinusoids are congested with blood cells (black stars) with apparent perisinusoidal fibrosis (F). The rest of the cell organelles are masked by the rarefied cytoplasm (right arrows). Mercury deposits appear within the cytoplasm (circles). (TEM ×10000)

Table 1: Body and liver weights.

	Body weight (g)			Liver weight (g)		
	Control (n = 6) Mean±SD	Treated (n=6) Mean±SD	*P value**	Control (n = 6) Mean±SD	Treated (n=6) Mean±SD	*P value**
GI	5.67 + 0.51	5.50+0.54	0.575	0.258 + 0.005	0.413 +0.003	0.004**
GII	48.67 + 2.34	38.0 + 2.82	0.004**	1.47 + 0.19	1.9 + 0.23	0.012**
GIII	219.17 + 15.60	175.33 + 6.	280.004**	4.93 + 0.38	10.23 + 2.87	0.004**

SD: Standard deviation. * Mann-Whitney Test. ** Statistically significant ($P < 0.05$).

Table 2: Hepatocytes nuclear diameter.

Hepatocytes nuclear diameter (µm)	Control (n = 6) Mean±SD	Treated (n=6) Mean±SD	*P value**
Group I	6.79 + 0.39	5.73 + 1.42	0.337
Group II	7.38 + 0.38	4.99 + 2.01	0.016**
Group III	7.29 + 0.59	6.04 + 0.56	0.006**

SD: Standard deviation. * Mann-Whitney Test. ** Statistically significant ($P < 0.05$).

DISCUSSION

Mercury is a prominent environmental contaminant that causes detrimental effects to the human health ***(Ung et al., 2010)***.

Group I

The present work revealed that the hepatic architecture of the treated livers was preserved comparative to the destructed outlines of the cells of the groups of the other ages. Hepatic nuclei were quite normal and the cytoplasm of the hepatocytes showed multiple vacuolated areas. These findings were previously described in Metwally *et al*. (2015) and Macirella *et al*. (2016) studies.

Infiltration of the inflammatory cells seen in the present work was a previous finding of studies of Begam and Sengupta (2015). It is well known that $HgCl_2$ treated tissues showed an up-regulation of pro-inflammatory cytokines ***(Begam and Sengupta, 2015)***. This can be evidenced by cell irritability, inflammation and hypersensitivity to the metal ***(Guzzi et al., 2008)***. Bile ductules were also observed surrounded by inflammatory cells in the present study and this could be referred to the extensive biliary-hepatic cycling ***(Andreoli and Sprovieri, 2017)***.

The present work exhibited large number of fat cells that appeared between the hepatocytes. This was with Ung *et al*. (2010) study on mercury-induced hepatotoxicity in Zebrafish. The researchers pointed to the increased number and size of the lipid vesicles detected in the liver of the treated fish.

The blood sinusoids appeared to be dilated and filled with haemopoietic cells in the present study which might indicate the haemopoietic function of the liver preserved from the prenatal life ***(Krishna, 2013)***. However, lymphocytic infiltration added to the sinusoidal blood congestion after treatment with a toxin, are positive indicators of the hepatic damage as mentioned by Liu *et al*. (2011) and Metwally *et al*. (2015).

The present work demonstrated that the vacuolization process of the cytoplasm started at the periphery. This was also stated in the work of Macirella *et al*. (2016). This might be ruled by formation of vacuolar structures that displayed very intensive fusion and fission activity especially at periphery of the cell ***(Bentov et al., 2009)***.

Apparent loss of the cell organelles was noticed in the present study and this was in agreement with the research of Vergilio *et al*. (2015). They mentioned that $HgCl_2$ treatment of the hepatocyte cultures has induced progressive structural damage which led to cell death. They declared that mercury reached several targets simultaneously. Persistent mitotic divisions of the hepatocytes seen in the present work might confirm cell integrity as the remaining cells grow to compensate for the mass of the tissue as reported by ***(Zaret and Grompe, 2008; Soto-Gutierrez et al., 2009)***.

The present work exhibited that $HgCl_2$ had the least degree of hepatic toxicity among rat fetuses. Jung-Duck and Wei (2012) studies pointed that

inorganic mercury salts as $HgCl_2$ are not lipid soluble and they theoretically do not cross the blood-placental barrier but the fetotoxic effect of $HgCl_2$ can be explained by the ability of the mercury to alter the membrane permeability without any loss in cell viability. Abboud and Wilkinson (2013) pointed that toxicity involves mercuric interaction with membrane thiols. Thus, during metal uptake from metal mixtures, mercury might promote the uptake of other toxic metals. As well, the high mobility of the mercury in the body might be due to the formation of water soluble mercury complexes which are attached to the sulfur atom of thiol groups such as glutathione ***(Jozefczak et al., 2012)***. The glutathione moiety is degraded in the bile duct and gall bladder of the pregnant rats and in the form of the L-cysteine complex, the mercury enters the endothelial cells of the placental barriers ***(Azevedo et al., 2012)***. Added to that the fetus is not able to excrete mercury ***(O`Reilly et al., 2010)***.

Group II

The swollen hepatocytes could be explained by the mercuric affection of the membrane permeability ***(Flora et al., 2008)***. Patchy necrotic areas had been detected within the hepatic lobules indicating marked affection of the liver tissue by the toxicity ***(Patnaik et al., 2010)***. This might be attributed to the possible role of early mercuric exposure in inducing oxidative stress mediated apoptosis ***(Morcillo et al., 2015A and 2015B)***.

Hepatic nuclei of the specimens of the present work were of different shapes and sizes which might be due to nuclear fragmentation as documented by Koff et al. (2015). The normally shaped hepatic nuclei of the present study showed ill-defined nucleoli. This might point to malfunction of nucleoli which could be the cause of hepatic cell disorders ***(Montanaro et al., 2008)***.

The blood appeared within the congested central veins as well as the congested dilated sinusoids that observed in the present study were supportive findings of the mercury produced hepatic congestion ***(Meng et al., 2012)***. Also, the presence of the densely infiltrated inflammatory cells supported the hepatic injury.

Prominent nuclei of von Kupffer cells seen in the present work could be attributed to the accumulated foreign mercury that might result in damage of the protein molecules of the cells thus leading to their disfigurement ***(Treesh et al., 2014)***.

Mitochondrial polymorphism seen in this age could be of insignificant value as the mitochondria vary with cell type, developmental stage and environment ***(Vafai and Mootha, 2012)***.

Mitotic divisions of the hepatocytes were present in this study might indicate integrity of some hepatocytes. The mild perisinusoidal fibrosis could be a result of the chronic liver exposure to the mercury. Hepatic fibrosis is a consequence of chronic liver injury that in turn leads to increased deposition of extracellular matrix in perisinusoidal and periportal spaces inducing fibrosis ***(Xu et al., 2014; Zhang et al., 2016)***.

In the present work, the $HgCl_2$ has a considerable toxic effect on group II as well as group I. It is well known that mothers consuming diet containing mercury pass the toxicant to the fetus and to the infants through the breast milk. The prenatal mercuric exposure was also suggested to lead to increased mercuric level in the breast milk ***(Li et al., 2014)***. Furthermore, Jan et al. (2015) found that heavy metals can bind to albumin and casein in the breast milk.

In the present work, the toxic effect of $HgCl_2$ on the breastfed rats suggested that this form of mercury found its way through the intestinal wall to be absorbed. The corrosive effect of mercury on the intestine might increase the permeability and, hence, the absorption with prolonged exposure ***(Robin, 2012)***. All, or most, of the ingested mercury which is absorbed into systemic circulation may be erroneous ***(Bradley et al., 2017)***. In addition, a substantial portion of mercury in the fetal liver is bound to metallothionein which plays an important role as a reservoir of mercury during the prenatal period ***(Bourdineaud et al., 2012)***.

Group III

The hepatocytes were swollen and irregular which was more marked than that of the previous groups. Hypetrophy of these cells might be due to the swelling of the intracellular structures ***(Pandey et al., 2008)*** or as a result of disturbances of membranes function ***(Abdelhalim and Jarrar, 2011)***.

The binucleated hepatocytes appeared in the present work might be finding of a normal hepatic tissues. However, binucleation might be also a consequence of the cell injury and a sort of chromosomes hyperplasia which is usually seen in the regenerating cells ***(Abdelhalim and Jarrar, 2011)***.

Vacuolated cytoplasm-a finding of the present study- might be of no significance if it is not accompanied with other hepatic changes. For example, the alterations in the amount of hepatocellular glycogen are frequently accompanied by cytoplasmic vacuolization. This was evidenced by the vacuolated cytoplasm in the Hx&E stained specimens of the controls in study of Thoolen *et al*. (2010) and Krishna (2013).

Thoolen *et al*. (2010) declared that in the absence of any treatment-related changes within a study, the degrees of glycogen demonstrated in the hepatocytes are considered as background changes. In contrast, when differences in the amount of glycogen amount are accompanied by other cytoplasmic changes, glycogen accumulation or depletion may not be easily discerned ***(Haschek et al., 2010)***.

Furthermore, this change was seen too in the current work by TEM of the control groups in which the gluteraldehyde fixation is accused with a considerable loss of glycogen in the tissues so, a mild vacuolization of the cells occurred ***(Bindhu et al., 2013)***.

On the other hand, the vacuolated swelling of the treated groups might indicate acute and subacute liver injury induced by the drug. This was in agreement with studies of Schrand *et al.* (2010) and Abdelhalim and Jarrar (2011). They postulated that the vacuolization might be a result of a hydropic degenerative process as a consequence of ion and fluid homestasis that led to an increase of intracellular water.

The central veins together with the hepatic sinusoids of the present work were irregular, dilated, congested with blood and also had a destructed endothelium. Sayed (2014) and Joshia *et al*. (2014) referred the vascular dilatation to the increased levels of prostaglandins that induce smooth muscle relaxation with subsequent vasodilatation. Choledocholithiasis could be the most possible cause of the dilated bile ductules ***(Holm and Gerke, 2010)*** as a consequence of the inflammatory process involved. Mild to moderate biliary hyperplasia may be considered adverse in the rat but potentially poses a risk for humans particularly if accompanied by evidence of hepatobiliary injury or functional compromise ***(James et al., 2014)***.

Large number of Ito cells appeared within the persinusodal spaces of the present study indicating the hepatic affection. This was in agreement of Moreira (2007) and Krizhanovsky *et al*. (2008) who declared that Ito cells are the main matrix-producing cells in the process of liver fibrosis.

In the present work, the presence of mitotic figures within some hepatocytes was indicator of integrity of some cells. This may be considered a form of regenerative process done by the hepatocytes to compensate for the loss in hepatocytes ***(Sayed, 2014)***.

Some hepatocytes of the present work were of thickened cell membranes but others were of thinned ones. These results further supported the hypothesis that inorganic mercury affects the cell membrane ***(Guo et al., 2013)***. Thickened membranes may result from deposition of fibrin materials. It was reported by Nyland *et al*. (2012) that chronic subcutaneous administration of inorganic mercury significantly exacerbated fibrosis of the cardiac cells of the mice. Furthermore, the thickening of the organic lining might have a defense mechanism against the pollutants ***(Frontalini et al., 2016)*** or might be the autoimmune complexes formed within the cell ***(Crowe et al., 2017)***.

On the other hand, the cells of the thin membranes might point to the degenerative changes affected the cell membranes due to the disturbance of their nutritional state ***(Tamás et al., 2014)*** especially when gathered with the other cytoplasmic changes. With the ability of the mercury to change the plasma membrane fluids like quality, the cell becomes stiffer and ages faster ***(Nabi , 2014)***.

Increased number of lysosomes seen in the present study was also an observation of Frontalini *et al*. (2016) study. The authors documented that mercury was responsible for promotion of the proliferation of lysosomes both in number and dimension as the mercuric nanoparticles were sequestered and accumulated by lysosomes ***(Gomiero et al., 2013)***.

In the present work, mitochondria were few, swollen and small sized. Similar findings were reported by ***(Sayed, 2014)***. Other studies have shown that mercury produces an imbalance between the reactive oxygen species (ROS) production and its clearance by the antioxidant system either in *vivo* ***(Cappello et al., 2016A, 2016B; Guardiola et al., 2016)*** or in *vitro* ***(Morcillo et al., 2015A, 2016, 2017A)***. Also, mercuric forms induce apoptosis by inhibiting mitochondrial function ***(Zheng et al., 2014)***. The

existence of close contacts between mitochondria and the endoplasmic reticulum raises the possibility that mercuric metabolites generated in the endoplasmic reticulum could reach the mitochondria ***(De Brito and Scorrano, 2010)***. However, this was against Macirella *et al*. (2016) who pointed that the increased mitochondrial count might be considered as an unspecific adaptive response to mercury rather than a general response of the tissue to the metal.

In addition, being a toxic element that accumulates during life ***(Houston, 2011)***, body stores of mercury from prenatal life and lactation period could be another factor for the exaggerated toxicity in treated adults. Potential interactions between toxic and essential metals are also possible ***(Jadhav et al., 2007)***. With those facts, such chronic toxicity can be easily explained.

The insignificant difference in the nuclear diameter between both control and treated livers of the present work groups correlates with the previous histological findings. In contrast, groups II and III showed significant reduction in the nuclear diameters indicating the nuclear shrinkage as mentioned by ***(Vergilio et al., 2015)***.

In the current study, $HgCl_2$ had a significant reduction in the weight of the rats of groups II and III. This comes in accordance with Necib *et al*. (2013). This drop in the body weight could be attributed to the general glycolytic state produced to meet the energy demands imposed by enhanced metabolic activity as reported by ***(Javed and Usmani, 2015)***. Recent studies by Morcillo *et al*. (2017B) suggested that an exposure to the dissolved mercury disrupts the epithelium that results in compensatory changes in ventilation frequency and increased energy demands resulting in the increase in metabolic rate.

The present work revealed that $HgCl_2$ toxicity was associated with a significant increase in the weight of the treated livers of the rats of group I, II and III. This comes in agreement with Necib *et al*. (2013). However, it was against Drevnick *et al*. (2008) and Macirella *et al*. (2016) studies. Drevnick *et al*. (2008) pointed to the decreased lipid reserves in livers of northern pike fish with high liver total mercury concentrations supposing that mercury has a lipolytic activity. Macirella *et al*. (2016) postulated that the decrease in lipid stores might suggest an increase of basal metabolic pathways of hepatocytes.

At the same time, the present work revealed a significant weaker PAS reaction of groups I and II indicating the glycolytic activity done by the liver under stress conditions produced by the toxicity ***(Javed and Usmani, 2015; Macirella et al., 2016)***. In general, the great loss of glycogen in the liver indicates that it is the most affected organ during stress as declared by George *et al*. (2012).

With the increase in the lipid material of the liver that overshot the decrease in the glycogen stores, the increase in the liver weight could be explained. However, added to the lipid deposition, the treated livers of the group III of the present work showed stronger PAS reaction than the control group. Ung *et al*. (2010) explained that by the disturbing effect of the mercury on the carbohydrates metabolism with the chronic exposure to the metal that led to accumulation of glycogen in the liver which together with the deposited lipid markedly elevated weight of the livers.

CONCLUSION

The $HgCl_2$ has injurious effect on the postnatally developing liver.

CONFLICT OF INTERESTS

There are no conflicts of interest.

REFERENCES

Abboud, P. and Wilkinson, K. 2013. Role of metal mixtures (Ca, Cu and Pb) on Cd bioaccumulation and phytochelatin production by Chlamydomonas reinhardtii. Environmental Pollution 179: 33-38.

Abdelhalim, M. and Jarrar, B. 2011. Gold nanoparticles induced cloudy swelling to hydropic degeneration, cytoplasmic hyaline vacuolation, polymorphism, binucleation, karyopyknosis, karyolysis, karyorrhexis and necrosis in the liver. Lipids Health Disease 10:166.

Andreoli, V. and Sprovieri, F. 2017. Genetic aspects of susceptibility to mercury toxicity: An Overview. International Journal of Environmental Research and Public Health 14(1): 93.

Azevedo, B., Furieri, L., Peçanha, F., *et al.* 2012. Toxic effects of mercury on the cardiovascular and central nervous systems. Journal of Biomedicine and Biotechnology 2012: 949048.

Begam, M. and Sengupta, M. 2015. Immunomodulation of intestinal macrophages by mercury involves oxidative damage and rise of pro-in flammatory cytokine release in the fresh water fish Channa punctatus Bloch. Fish& Shellfish Immunology 45(2): 378-385.

Bentov, S., Brownlee, C. and Ereza, J. 2009. The role of seawater endocytosis in the biomineralization process in calcareous foraminifera. Geology, Cell Biology 106(51): 21500-21504.

Bindhu, P., Krishnapillai, R., Thomas, P. and Jayanthi, P. 2013. Facts in artifacts. Journal of Oral Maxillofacial Pathology 17(3): 397-401.

Blum, J. 2013. Mesmerized by mercury. Nature Chemistry 5:1066.

Bourdineaud, J., Laclau, M., Maury-Brachet, *et al.* 2012. Effects of methylmercury contained in a diet mimicking the Wayana Amerindians contamination through fish consumption: Mercury Accumulation, metallothionein induction, gene expression variations, and role of the chemokine CCL2. International Journal of Molecular Sciences 13(6): 7710-7738.

Bradley, M., Barst, B. and Basu, N. 2017. A review of mercury bioavailability in humans and fish. International Journal of Environmental Research and Public Health 14(2): E169.

Cappello, T., Brandão, F., Guilherme, S., *et al.* 2016 A. Insights into the mechanisms underlying mercury-induced oxidative stress in gills of wild fish (Liza aurata) combining 1H NMR metabolomics and conventional biochemical assays. Science of the Total Environment 548-549: 13-24.

Cappello, T., Pereira, P., Maisano, M., *et al.* 2016 B. Advances in understanding the mechanisms of mercury toxicity in wild golden grey mullet (Liza aurata) by 1H NMR-based metabolomics. Environmental Pollution 219: 139-148.

Crowe, W., Allsopp, P., Watson, G, *et al.* 2017. Mercury as an environmental stimulus in the development of autoimmunity- a systematic review. Autoimmunity Reviews 16(1): 72-80.

De Brito, O. and Scorrano, L. 2010. An intimate liaison: Spatial organization of the endoplasmic reticulum-mitochondria relationship. European Molecular Biology Organization Journal 29(16): 2715-2723.

Drevnick, P., Roberts, A., Otter, R., *et al.* 2008. Mercury toxicity in livers of northern pike (Esox lucius) from Isle Royale, USA. Comparative Biochemistry and Physiology Part C: Toxicology & Pharmacology 147 (3): 331-338.

Flora, S. Mittal, M. and Mehta, A. 2008. Heavy metal induced oxidative stress & its possible reversal by chelation therapy. Indian Journal of Medical Sciences 128(4): 501-523.

Frontalini, F., Curzi D., Cesarini E., *et al.* 2016. Mercury-pollution induction of intracellular lipid accumulation and lysosomal compartment amplification in the Benthic Foraminifer Ammonia parkinsoniana. PLoS One 11 (9): e0162401.

George, K., Malini, N. and Rani, G. 2012. Biochemical changes in liver and muscle of the cichlid, Oreochromis mossambicus (Peters, 1852) exposed to sub-lethal concentration of mercuric chloride. Indian Journal of Fisheries 59: 147-152.

Gomiero, A., Dagnino, A., Nasci, C. and Viarengo, A. 2013. The use of protozoa in ecotoxicology: Application of multiple endpoint tests of the ciliate E. crassus for the evaluation of sediment quality in coastal marine ecosystems. Science of the Total Environment 442: 534-544.

Guardiola, F., Chaves-Pozo, E., Espinosa, C., *et al.* 2016. Mercury accumulation, structural damages, and antioxidant and immune status changes in the gilthead seabream (Sparus aurata L.) exposed to methylmercury. Archives of Environmental Contamination and Toxicology 70(4): 734-746.

Guo, B., Yan, C., Cai, S., Yuan, X. and Shen, X. 2013. Low level prenatal exposure to methylmercury disrupts neuronal migration in the developing rat cerebral cortex. Toxicology 304: 57-68.

Guzzi, G. and La Porta, C. 2008. Molecular mechanisms triggered by mercury. Toxicology 244(1): 1-12.

Guzzi, G., Pigatto, P., Minoia, C., *et al.* 2008. Dental amalgam, mercury toxicity and renal autoimmunity. Journal of Environmental Pathology, Toxicology and Oncology 27 (2): 147-155.

Haschek, W., Rousseaux, C. and Wallig, M. 2010. Fundamentals of toxicologic pathology, 2nd ed. Academic Press, San Diego, 197-235.

Holm, A. and Gerke, H. 2010. What should be done with a dilated bile duct. Current Gastroenterology Reports12 (2):150-156.

Houston, C. 2011. Role of mercury toxicity in hypertension, cardiovascular disease, and stroke. The Journal of Clinical Hypertension 13 (8): 621-627

Jadhav, S., Sarkar, S., Aggarwal, M. and Tripathi, H. 2007. Induction of oxidative stress in erythrocytes of male rats subchronically exposed to a mixture of eight metals found as groundwater contaminants in different parts of India. Archives of Environmental Contamination and Toxicology 52: 145-151.

James, R., Nold, J., Brown, R., *et al.* 2014. Biliary proliferative lesions in the Sprague-Dawley rat. Adverse/Non-adverse. Toxicological pathology 42 (5): 844-854.

Jan, A., Azam, M., Siddiqui, K., *et al.* 2015. Heavy metals and human health: mechanistic insight into toxicity and counter defense system of antioxidants. International Journal of Molecular Sciences 16(12): 29592-29630.

Javed, M. and Usmani, N. 2015. Impact of heavy metal toxicity on hematology and glycogen status of fish: A Review. Springer 85 (4): 889-900.

Joshia, D., Mittal, D., Shukla, S., *et al.* 2014. N-acetyl cysteine and selenium protects mercuric chloride-induced oxidative stress and antioxidant defense system in liver and kidney of rats: A histopathological approach. Journal of Trace Elements in Medicine and Biology 28(2): 218-226.

Jozefczak, M., Remans, T., Vangronsveld, J. and Cuypers, A. 2012. Glutathione is a key player in metal-induced oxidative stress defenses. International Journal of Molecular Sciences 13(3): 3145-3175.

Jung-Duck, P. and Wei, Z. 2012. Human exposure and health effects of inorganic and elemental mercury. Journal of Preventive Medicine & Public Health 45 (6): 344 - 352.

Koff, J., Ramachandiran, S. and Bernal-Mizrachi, L. 2015. A time to kill: Targeting apoptosis in cancer. International Journal of Molecular Sciences 16(2): 2942-2955.

Krishna, M. 2013. Microscopic anatomy of the liver (review). Clinical Liver Disease 2, No. S1.

Krizhanovsky, V., Yon, M., Dickins, R., *et al.* 2008. Senescence of activated stellate cells limits liver fibrosis. Cell 134 (4): 657-667.

Kue, J. 2007. Electron microscopy methods and protocols. New Jersey. Springer. Science & Business Media 3:1-8.

Kyriacos, A., Athanasiou L., Darling, M., *et al.* 2013. Articular cartilage. CRC Press. P: 331.

Levesque, R. 2007. SPSS programming and data management: A guide for SPSS and SAS users, Fourth Edition.

Li, M., Wu, M., Xu, J., *et al.* 2014. Body burden of Hg in different bio-samples of mothers in Shenyang City, China. PLoS ONE 9(5): e98121.

Liu, C.; Ma, J. and Sun, Y. 2011. Protective role of puerarin on lead induced alterations of the hepatic glutathione antioxidant system and hyperlipidemia in rats. Food and Chemical Toxicology 49: 3119-3127.

Liu, G., Cai, Y., O'Driscoll, N., Feng, X. and Jiang, G. 2012. Overview of mercury in the environment. Environmental Chemistry and Toxicology of Mercury. 1st ed. John Wiley & Sons; Hoboken, NJ, USA P: 1-12.

Macirella, R., Guardia, A., Pellegrino, D., *et al.* 2016. Effects of two sublethal concentrations of mercury chloride on the morphology and metallothionein activity in the liver of zebrafish (Danio rerio). Internationale Journal of Molecular Science 17(3): 361.

Mahmoud, F. and El-Badry, M. 2001. Histological effects of gentamicin intaking during pregnancy on liver and kidney of fetus and mother of albino rat. Egyptian Journal of Anatomy 24(1): 35-57.

Meng, F., Wang, K., Aoyama, T., *et al.* 2012. Interleukin-17 signaling in inflammatory, Kupffer cells and hepatic stellate cells exacerbates liver fibrosis in mice. Gastroenterology 143(3): 765-776.

Metwally, E., Negm, F., Shams El-din, *et al.* 2015. Anatomical and histological study of the effect of lead on hepatocytes of Albino rats. International Journal of Biomedical Materials Research 3 (4): 34-45.

Mohamed, E., Mahran, H. and Mahmoud, M. 2010. Hepato-ameliorative effect of Azadirachta Indica leaves extract against mercuric chloride environmental pollution. American Science 6(9): 735-751.

Montanaro, L., Treré, D. and Derenzini, M. 2008. Nucleolus, ribosomes and cancer. American Journal of Pathology 173(2): 301-310.

Morcillo, P., Chaves-Pozo, E., Meseguer, J., *et al.* 2017 A. Establishment of a new teleost brain cell line (DLB-1) from the European Sea Bass and its use to study metal toxicology. Toxicology In *Vitro* 38: 91-100.

Morcillo, P., Cordero, H., Meseguer, J., *et al.* 2015 A. Toxicological in *vitro* effects of heavy metals on gilthead seabream (Sparus aurata L.) head-kidney leucocytes. Toxicology In *Vitro* 30(1): 412-420.

Morcillo, P., Cordero, H., Meseguer, J., *et al.* 2015 B. In *vitro* immunotoxicological effects of heavy metals on European sea bass (Dicentrarchus labrax L.) head-kidney leucocytes. Fish &Shellfish Immunology 47: 245-254.

Morcillo, P., Esteban, M. and Cuesta, A. 2017 B. Mercury and its toxic effects on fish. AIMS Environmental Science 4(3): 386-402.

Morcillo, P., Esteban, M. and Cuesta, A. 2016. Heavy metals produce toxicity, oxidative stress and apoptosis in the marine teleost fish SAF-1 cell line. Chemosphere 144: 225-233.

Moreira, R. 2007. Hepatic stellate cells and liver fibrosis. Archives of Pathology & Laboratory Medicine 131(11): 1728-1734.

Nabi, S. 2014. Toxic effect of mercury. Springer science and business media 1: 237.

Necib, Y., Bahi, A., Zerizer, S., *et al.* 2013. Hepatoprotective role of sodium selenite against oxidative damage induced by mercuric chloride in rat Albinos Wistar. Journal of Stress Physiology & Biochemistry 9 (4): 230-240.

Nyland, J., Fairweather, D., Shirley, D., *et al.* 2012. Low dose inorganic mercury increases severity and frequency of chronic Coxsackievirus-induced autoimmune myocarditis in Mice. Toxicological Sciences 125 (1): 134-143.

O`Reilly, B., McCarty, K., Steckling, N. and Lettmeier, B. 2010. Mercury exposure and children health. Current Problems in Pediatric and Adolescent Health Care 40(8): 186-215.

Pandey, G., Srivastava, D. and Madhuri, S. 2008. Standard hepatotoxic model produced by paracetamol in rat. Toxicology International 15(1): 69-70.

Patnaik, B., Roy, A., Agarwal, S. and Bhattacharya, S. 2010. Induction of oxidative stress by non-lethal dose of mercury in rat liver: Possible relationships between apoptosis and necrosis. Journal of Environmental Biology 31(4): 413-416.

Rastogi, R. 2009. Practical zoology. New Delhi, India. Rajpal And Sons Publishing 8 : 3.

Robin, A. 2012. Mercury toxicity and treatment: A review of the literature. Journal of Environmental and Public Health 2012; 1-10.

Rui, L. 2014. Energy metabolism in the liver. Comprehensive Physiology 4(1): 177-197.

Rustagi, N. and Singh, R. 2010. Mercury and health care. Indian Journal of Occupational and Environmental Medicine 14(2): 45-48.

Sayed, H. 2014. The effect of mercuric chloride on the liver of male albino rat and possible protective role of selenium; Histomorphological and ultrastructural study. Thesis submitted for M.D degree in Anatomy Faculty of Medicine , Cairo University.

Schrand, A., Rahman, M., Hussain, S., et al. 2010. Metal-based nanoparticles and their toxicity assessment. Nanomedicine and Nanobiotechnology 2: 544-568.

Soto-Gutierrez, A., Navarro-Alvarez, N., Yagi, H. and Martin, L. 2009. Stem cells for liver repopulation. Current Opinion in Organ Transplantation 14(6): 667-673.

Tamás, M., Sharma, S., Ibstedt, S., *et al.* 2014. Heavy metals and metalloids as a cause for protein misfolding and aggregation. Biomolecules 4: 252- 267.

Tayeb, K., Lemaigre, F. and Duncan, S. 2010. Organogenesis and development of the liver. Developmental Cell 18(2):175-189.

Thoolen, B., Maronpot, R., Harada, T., *et al.* 2010. Hepatobiliary lesion nomenclature and diagnostic criteria for lesions in rats and mice (INHAND). Toxicologic Pathology 38: 5S-81S.

Treesh, S., Eljaafari, H., Darmun, E., *et al.* 2014. Histological study on the effect of formaldehyde on mice liver and kidney and possible protective role of selenium. Journal of Cell and Tissue Research 14(2): 4201-4209.

Ung, C., Lam, S., Hlaing, M., *et al.* 2010. Mercury induced hepatotoxicity in zebrafish. BMC Genomics 30(11): 212.

Vafai, S. and Mootha, V. 2012. Mitochondrial disorders as windows into an ancient organelle. Nature 491(7428): 374-383.

Vergilio, C., Carvalhob, C., and Meloa, E. 2015. Mercury induced dysfunctions in multiple organelles leading to cell death. Toxicology in *Vitro* 29(1): 63-71.

Xu, J., Liu, X., Koyama, Y., *et al.* 2014. The types of hepatic myofibroblasts contributing to liver fibrosis of different etiologies. Front Pharmacol 5: 167.

Zaret, K. and Grompe, M. 2008. Generation and regeneration of cells of the liver and pancreas. Science 322(5907):1490-1494.

Zhang, C., Yuan, W., He, P., *et al.* 2016. Liver fibrosis and hepatic stellate cells: Etiology, pathological hallmarks and therapeutic targets. World Journal of Gastroenterology 22(48): 10512-10522.

Zheng, G., Liu, C., Sun, J., *et al.* 2014. Nickel-induced oxidative stress and apoptosis in Carassius auratus liver by JNK pathway. Aquatic Toxicology 147: 105-111.

تأثيرالتعرض لمادة كلوريد الزئبق أثناء فترتي الحمل والرضاعة علي نمو الكبد في الفأرالأبيض خلال مرحلة ما بعد الولادة

محمد البدري محمد أحمد، منال محمود سامي أحمد المليجي، رينيه رفعت بشري تادرس، إسراء خالد محمد نفادي
قسم التشريح الآدمي وعلم الأجنة، كلية الطب – جامعة أسيوط

ملخص البحث

مقدمة: يعد الزئبق أحد الملوثات البيئية في الوقت الراهن والتي تسبب أضراراً جسيمة لصحة الإنسان؛ يتم التعرض لمادة الزئبق من خلال استخدام المعدات المحتوية عليه في تركيبها الكيميائي مثل: البطاريات, الترمومترات الزئبقية، الدهانات، الأجهزة الكهربائية، المصابيح المشعة، المبيدات الحشرية، وبعض أدوات التجميل كالماسكارا، كما يستخدم أيضا في العديد من المجالات الطبية مثل : حشوة الأسنان الفضية، المطهرات الموضعية، بعض الأدوية الملينة، مراهم تفتيح البشرة و رذاذات الأنف والعين.
الهدف: دراسة تأثيرالتعرض لمادة كلوريد الزئبق أثناء فترتي الحمل والرضاعة علي نمو الكبد في الفأرالأبيض خلال مرحلة ما بعد الولادة .
الوسائل والطرق: تم استخدام عدد 20 فأر أبيض بالغ؛ 16 أنثي و4 ذكور, تم السماح بالتزاوج وتسجيل حدوث الحمل. تم تقسيم الإناث الحوامل إلي مجموعتين: المجموعة الضابطة (8 فئران) والمجموعة المعالجة (8 فئران). عولجت المجموعة الضابطة بمحلول ملحي عن طريق الفم يومياً باستخدام الأنبوبة المعدية في حين أعطيت المجموعة المعالجة مادة كلوريد الزئبق بجرعة 2 مجم/كجم من وزن الجسم. بعد انتهاء فترة الرضاعة أعطيت ذرية المجموعة المعالجة مادة كلوريد الزئبق بنفس الجرعة السابقة يوميا. تمت التضحية بذرية كلتي المجموعتين في الأعمار الآتية: يوم، واحد وعشرون يوماً, شهرين حيث تم تمثيل كل عمر بعدد 12 فأر (6 فئران ضابطة و 6 فئران معالجة)، تم استخراج الكبد وتحضيره للفحص المجهري الضوئي والإلكتروني. وتم عمل بعض القياسات المورفوميترية.
النتائج: التعرض لمادة كلوريد الزئبق يؤدي الي حدوث أضرار جسيمة بالكبد علي كافة الأعمار قيد الدراسة، وعلي كافة المستويات التركيبية والخلوية والوعائية الدموية، فقد أوضح الميكروسكوب الضوئي حدوث تخلخل في السيتوبلازم واختلال في الهندسة التركيبية للخلايا الكبدية، بالاضافة إلى حدوث اتساع واحتقان في الجيبيبات الدموية واحتقان في الأوردة المركزية وجذيريات الوريد البابي الكبدي، وأسفرعن ظهور واضح للخلايا الالتهابية، وأيضا نقص في الجليكوجين داخل خلايا الكبد فيما يخص المجموعتين الاولي والثانية وعلي نقيض المجموعة الثالثة. وأظهرت خلايا الثلاث مجموعات المعالجة وجود انحدار واضح في عدد الميتوكوندريا وتخلخل في السيتوبلازم، بالإضافة إلي ظهور بعض الأنسجة الضامة والتليفات خاصة حول الجيبيبات الدموية، كما وجد نقص في أوزان أجسام الفئران المعالجة بينما زادت أوزان أكبادها.
الاستنتاج: أن الزئبق له تأثير ضار علي الصحة.